IEEE Access
Multidisciplinary | Rapid Review | Open Access Journal

Received July 10, 2020, accepted July 14, 2020, date of publication July 17, 2020, date of current version July 28, 2020.

Digital Object Identifier 10.1109/ACCESS.2020.3010047

Optimal Pulse Shifting in Timed Antenna Array for Simultaneous Reduction of Sidelobe and Sideband Level

AVISHEK CHAKRABORTY[1], (Graduate Student Member, IEEE), GOPI RAM[2], AND DURBADAL MANDAL[1], (Member, IEEE)

[1]Department of Electronics and Communication Engineering, National Institute of Technology, Durgapur 713209, India
[2]Department of Electronics and Communication Engineering, National Institute of Technology, Warangal 506004, India

Corresponding author: Gopi Ram (gopi.ram@nitw.ac.in)

This work was supported by the Department of Science and Technology, Science and Engineering Research Board (SERB), Government of India, under Grant EEQ/2017/ 000519 (dated 23.03.2018).

ABSTRACT Optimal pulse shifting in timed antenna array for the reduction of sidelobe and sideband using improved harmony search algorithm (IHSA) dealt in this paper. The essence of 'Time-modulation' lies in the fact that 'Time' can be used as an additional control parameter in antenna array synthesis. The proposed approach demonstrates the controlling nature of periodic time sequences through pulse shifting. The undesired sideband radiations (SRs) generated in time modulated linear array (TMLA) is controlled by minimizing the sideband levels (SBLs) with an optimal pulse shifting scheme applied to the outer elements of the array. Evolutionary algorithm-based design is considered to optimize the time sequences and the excitation coefficients of the array along with the inter-element spacing between the array elements for sidelobe level (SLL) reduction at the fundamental frequency. Pulse shifting with optimized switch-ON instants and switch-ON time intervals of outer elements is responsible for the minimization of SBL only, as the fundamental pattern does not depend on pulse shifting. Thus, a combined approach is developed with optimized excitation coefficients and controlled pulse switching to reduce the SLL and SBL of TMLA simultaneously. 16 and 30 isotropic elements of TMLA structures are considered with a music-inspired IHSA to get the optimal solution. IHSA based numerical results are compared with the results obtained from other applied algorithms such as harmony search algorithm (HSA), particle swarm optimization (PSO), and real-coded genetic algorithm (RGA) with the proposed pulse shifting scheme. The obtained numerical results are also compared with previously published literature results to show the superior performance achieved by the proposed approach.

INDEX TERMS Genetic algorithms, harmony search algorithms, improved harmony search algorithms, particle swarm optimization, pulse shifting, sidelobe level, sideband level, time-modulation.

I. INTRODUCTION

Single element antenna usually has a wide radiation pattern with low directivity. For long-distance communication, highly directive radiation patterns are required. Directivity or gain can be enhanced by increasing the electrical size of the antenna or by arranging multiple radiating elements in a specific electrical or geometrical configuration, acting as an array [1]. Fields from multiple radiating elements add constructively in the desired direction and destructively in all other directions to form a highly directive main beam. Synthesis of conventional antenna array with specific element positions, optimally weighted amplitude distribution, and phase excitations can achieve multiple objectives such as beam shaping, placing nulls, low/ultra-low SLL, etc. [2]. But the conventional array synthesis methods suffer from large dynamic range ratio (DRR) for which precise error tolerance is required. Phase shifters used to control the phase excitations of each element, also have high insertion loss and quantization errors. Furthermore, the complexity of the array feeding network also increases with attenuators and phase shifters for each element. To get the better of these problems,

The associate editor coordinating the review of this manuscript and approving it for publication was Diego Oliva.

a fourth dimension – 'Time' is introduced as an additional control parameter by Shanks *et al.* in 1959 [3]. The basic idea behind 'Time-modulation' is the variation of excitations as a function of time in a periodical manner, to produce the desired time-averaged radiation pattern. Periodically modulated excitations or suitable time sequences can be generated with simple ON-OFF switching of array elements by a set of high-speed radio-frequency (RF) switches in a stipulated manner. The additional degree of freedom comes with the inherent problem of undesired SR, as a portion of the radiated or received energy is shifted at multiples of the modulation frequency (harmonic frequency) due to periodical commutation of the switching device. Following the idea of time modulation, Kummer *et al.* realized an ultra-low SLL using time modulated receiving array with slot radiators [4]. In addition to sidelobe suppression, the concept of fourth dimensional (4D) array also becomes relevant to multipattern operation and electronic scanning [5]. Yang *et al.* first reported the suppression of SR by lowering the SBL with optimized static amplitude excitation and switch-ON time instants [6]. The research on time-modulated antenna arrays (TMAAs) has gained acceleration with the emergence of evolutionary optimization algorithms. Comparative studies have shown that low/ultra-low SLL can be achieved by uniformly as well as a non-uniformly excited array with adjustable switching sequences [7]. Both, equally and unequally spaced linear array with static excitation are presented for broadband response [8]. The exploitation of different time schemes with quantized time steps optimized directly via an evolutionary algorithm has found suitable applications in lowering the SLL and SBL simultaneously [9]. Synthesis of sum and difference patterns [10], as well as shaped pattern synthesis [11], opened up the possibilities to use TMAA in emerging fields such as radar tracking system [12], direction-finding [13], the direction of arrival estimation [14], beam steering [15] and so on. Unwanted SR generally considered as a loss of radiated energy, but in some instances, it is used on purpose to get the steered multi-beam pattern [16], which enhances the potentialities of TMAA in harmonic beamforming application [17]. Evolutionary algorithm-based designs have also considered for various applications such as directivity maximization [18], multiple broad nulls [19], and null synthesis [20], which implies the applicability of TMAA in point to point communication with interference rejection.

Several research works have been proposed using unequally spaced elements [21] or partially thinned elements [22] to suppress the unwanted radiation in harmonics. The concept of pulse shifting first appeared in the beam steering application [15]. The mathematical proof shows that SBL can be controlled with optimized switch-ON instants and switch-ON intervals without affecting the SLL, as the fundamental pattern does not depend on pulse shifting [23], [24]. The pulse or the time sequence of each element within the stipulated modulation period is shifted in a rotational manner such that they are divided into sub-sectional time steps keeping the total switch-ON time constant [25]. Pulse splitting with binary optimized time sequence [9] and pulse shifting under static fundamental radiation have also improved the SBL suppression [26]. Sideband reduction has also been reported with isotropic linear and planar arrays [27] as well as directive linear array based on the optimization of pulse sequence [28].

Time Modulated Linear Arrays (TMLAs) have shown radical improvements over the conventional linear antenna arrays in achieving ultra-low or nearly ultra-low SLL, which is suitable for leading-age applications like radar communication, interference rejection for the cluttered environment, and highly secure point-to-point and multi-point signal transmission. The challenges that need to be addressed for these applications are SLL reduction, SBL suppression, directivity improvement, and maintaining a pointed main beam pattern with narrower beamwidth. Published works on TMLAs have addressed these issues with distinct approaches [29]. Most of the literature has considered conventional methods such as Chebyshev or Taylor to produce -30 dB SLL and then tried to reduce the SBLs through different approaches based on some suitable optimization strategy. In some literature, analytical techniques have also been developed to reduce the SBLs instead of using optimization techniques. Apart from that, some research also shows a combined approach to reduce the SLL and SBLs in such a way that a balanced result between these two can be achieved. Due to the conflicting nature, low or nearly ultra-low SLLs and SBLs have been achieved with these methods, so far. The scope of improvement in simultaneous reduction of SLL and SBLs along with narrower beamwidth to produce a highly directive main beam is still a serious research concern for TMLA. This paper has addressed these challenging issues with a unique approach of controlling the outer elements of the array through an optimized pulse shifting strategy. The proposed approach has also managed to achieve a narrower main beam, with an enhancement in directivity in comparison to the already published works. Furthermore, only four outer elements are considered for optimized pulse shifting, which implies that the complexity of the switching network is also reduced as a lesser number of switches are required to be controlled.

The proposed approach has exploited evolutionary optimization techniques to generate the desired array patterns. The excitation coefficients of each element and the switch-ON intervals (the ON-time duration) of outer elements along with the inter-element spacing between them are optimized to get the ultra-low SLL for the fundamental pattern. The optimized ON-time durations (pulses) of outer elements are shifted based on the optimized switch-ON instants within the stipulated modulation period to reduce the SBL. TMLA structures of 16 and 30 isotropic elements are considered in this paper with an optimal pulse shifting scheme.

Due to the emergence of advanced meta-heuristics and their new variants in recent years, evolutionary algorithms have become more imperative to multi-disciplinary research [30], [31]. Numerous applications of evolutionary algorithms can also be found in the field of antenna

array synthesis [32]–[38]. These algorithms can produce near-global optimum solutions for a particular problem based on a suitable objective function. In the proposed approach, multiple objectives have been taken care of using a single objective optimization with appropriate weighting factors. For this problem, IHSA is performing better than all other opted algorithms to achieve an optimal solution due to its superior exploitative and explorative properties. For a fair comparison, results obtained from IHSA, HSA, PSO, and RGA are presented. Nature of ultra-low SBLs up to the first twenty positive harmonics and ultra-low SLLs obtained from different optimization techniques are compared with already published results.

The rest of the paper is organized as follows: In Section II, the theoretical background of TMLA is summarized along with the design equations. Evolutionary algorithms applied for the proposed work are covered in Section III. Section IV deals with numerical results, comparisons, and analysis of the results. In section V, convergence profiles obtained for applied algorithms are discussed in detail. Finally, the conclusive statements are presented in Section VI.

II. THEORY AND DESIGN EQUATION

Consider a linear antenna array of N equally spaced isotropic elements, directed along the positive z-axis, shown in Fig. 1. The far-field radiation pattern of the array, proportional to the weighted sum of the received signal from each element, can be expressed as

$$AF\ (\theta) = \sum_{n=1}^{N} I_n e^{jk(n-1)dcos\theta} \tag{1}$$

where I_n is the amplitude excitation of the n^{th} element, k is the propagation constant, d is the spacing between radiating elements, θ denotes the angle measured from the array main axis, and the phase excitations are considered to be identical.

Each element of the time-modulated array is assumed to be connected with a high-speed RF switch, shown in Fig. 2. Considering all excitations to be real, the time-dependent expression of the array factor can be modified from Eq. (1) as [6]

$$AF(\theta, t) = e^{j(2\pi f_0)t} \sum_{n=1}^{N} I_n U_n(t) e^{jk(n-1)dcos\theta} \tag{2}$$

The array is operating at fundamental frequency f_0 (in GHz), with T_0 being the fundamental period. The switching function $U_n(t)$ is periodic in nature with time-modulation frequency f_p (in MHz), which is much smaller than the fundamental frequency f_0 (i.e., $f_p \ll f_0$ and $T_p \gg T_0$) where T_p is the period of modulation). Due to the periodical nature of the switching function, it can be decomposed into the frequency domain as

$$U_n(t) = \sum_{m=-\infty}^{\infty} a_{mn} e^{jm(2\pi f_p)t} \tag{3}$$

where a_{mn} denotes the Fourier excitation coefficient of n^{th} element for the m^{th} order frequency component ($m = 0, \pm1, \pm2, \pm3, \ldots. \pm\infty$), can be obtained from

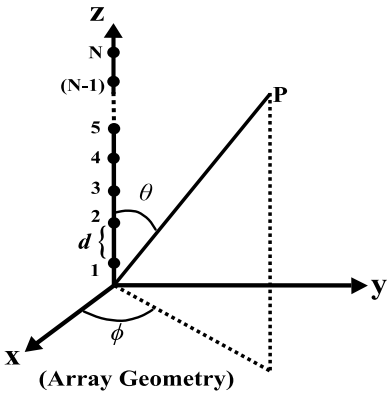

FIGURE 1. The geometry of N-element isotropic TMLA.

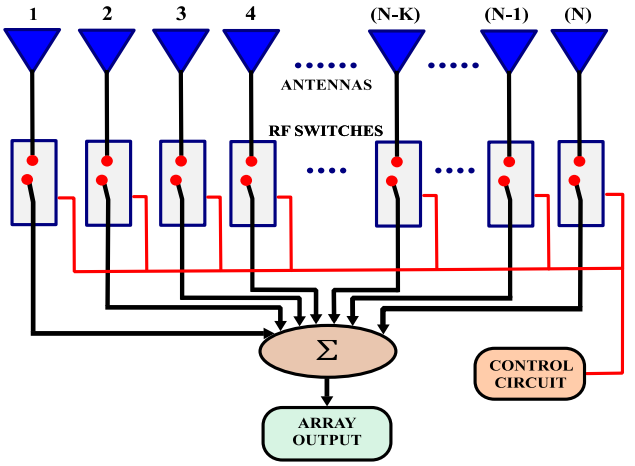

FIGURE 2. Generalized N-element TMLA configuration with switches.

equation (3) as

$$a_{mn} = \frac{1}{T_p} \int_0^{T_p} U_n(t) e^{-jm(2\pi f_p)t} dt \tag{4}$$

Here, $m = 0$ represents the fundamental frequency, and $m = \pm1, \pm2, \pm3, \ldots. \pm\infty$, represent the harmonic components. Combining Eq. (2) and the periodic switching function of Eq. (3), the time-dependent array factor becomes

$$AF(\theta, t) = \sum_{m=-\infty}^{\infty} \sum_{n=1}^{N} a_{mn} \{e^{jk(n-1)dcos\theta}\} e^{j2\pi(f_0+mf_p)t} \tag{5}$$

The expression of array factor in Eq. (5) can further be simplified for the m^{th} order harmonic frequency as

$$AF_m(\theta, t) = e^{j2\pi(f_0+mf_p)t} \sum_{n=1}^{N} I_n a_{mn} e^{jk(n-1)dcos\theta} \tag{6}$$

The radiation pattern of $(f_0 + f_p)$ at $m = 1$ and $(f_0 + 2f_p)$ at $m = 2$ represent the first two positive sidebands of the array with the fundamental frequency component at f_0 ($f_0 \gg f_p$). The directivity of the time-modulated linear array can be expressed as [39]

$$D = \frac{|AF_0(\theta_0, \phi_0)|^2}{\frac{1}{4\pi} \sum_{m=-\infty}^{\infty} \int_0^{2\pi} \int_0^{\pi} |AF_m(\theta, \phi)|^2 sin\theta d\theta d\phi} \tag{7}$$

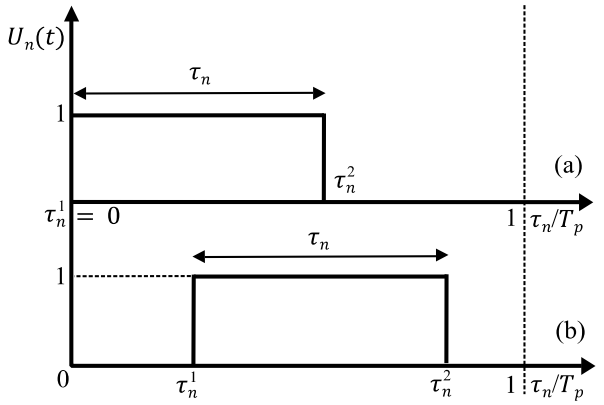

FIGURE 3. Time schemes (a) without shifted pulse, and (b) with shifted pulse configuration for TMLA.

where the main lobe of the fundamental radiation pattern ($m = 0$) is pointing at $\theta = \theta_0$, $\phi = \phi_0$, direction and $AF_m(\theta, \phi)$ is the radiation pattern at m^{th} harmonic frequency with an isotropic point source.

A. PULSE SHIFTING

The switching function $U_n(t)$ can be expressed with different time schemes for different TMLA applications, but they must be periodic in nature. The proposed work is focused on controlling the outer elements of the array with pulse shifting within the modulation period T_p to get the desired radiation pattern. The switching scheme is shown in Fig. 3, and the time switching function can be expressed as

$$U_n(t) = \begin{cases} 1, & 0 \le \tau_n^1 \le t \le \tau_n^2 \le T_p \\ 0, & otherwise \end{cases} \tag{8}$$

The switch-ON time for the n^{th} element of the array is presented as τ_n within the modulation period T_p ($0 \le \tau_n \le T_p$), and the normalized ON-time duration for the n^{th} pulse can be expressed as τ_n/T_p. The normalized pulse, starting from 0 (without shift), is presented in Fig. 3(a), and the same pulse is shifted in Fig. 3(b) within the modulation period. The shifted pulse is starting from τ_n^1 and ending at τ_n^2 with normalized ON-time duration of $\{(\tau_n^2 - \tau_n^1)/T_p\}$.

Considering nonuniform amplitude excitation ($I_n \neq 1$) for each element of the array and shifted pulse shown in Fig. 3(b), the Fourier excitation coefficient a_{mn} can be determined as

$$a_{mn} = \frac{1}{T_p}\int_{\tau_n^1}^{\tau_n^2} U_n(t) e^{-jm(2\pi f_p)t}\, dt \tag{9}$$

$$= I_n f_p(\tau_n^2 - \tau_n^1)\frac{[sin\{m\pi f_p(\tau_n^2 - \tau_n^1)\}]}{[m\pi f_p(\tau_n^2 - \tau_n^1)]} e^{-jm\pi f_p(\tau_n^1 + \tau_n^2)} \tag{10}$$

$$= \frac{I_n(\tau_n^2 - \tau_n^1)}{T_p}[sinc\{m\pi f_p(\tau_n^2 - \tau_n^1)\}] e^{-jm\pi f_p(\tau_n^1 + \tau_n^2)} \tag{11}$$

Equation (11) represents the shifted pulse sequence Fig. 3(b). In this proposed approach, the outer elements of the linear TMLAs are considered for pulse shifting, and for all other elements, the normalized switch-ON times are predefined as $\{(\tau_n^2 - \tau_n^1)/T_p\} = 1$. The generalized expression of a_{mn} for the m^{th} harmonic without pulse shifting can be derived as

$$a_{mn} = \frac{I_n \tau_n}{T_p}\{sinc(m\pi f_p \tau_n)\} e^{-jm\pi f_p(\tau_n)} \tag{12}$$

The Fourier coefficient of fundamental component ($m = 0$) is given as $a_{0n} = I_n \tau_n / T_p$. This shows that the fundamental pattern is not affected by pulse shifting, as it only depends on the normalized ON-time duration and amplitude excitation of each element. But, the undesired radiation pattern at harmonic frequencies depends on both the switch-ON instants and the switch-ON intervals.

B. COST FUNCTION

The power associated with sidebands is generally considered as losses. The realization of ultra-low SLL at the fundamental pattern, and a simultaneous reduction in SBLs at harmonics, can be cast into an optimization problem. SLL of the fundamental pattern can be minimized by optimizing excitation amplitudes and normalized ON-time pulses of each element. SRs can be averaged over the whole angle of arrival region of the array, as uniformly as possible, with optimized pulse shifting. Here, four outer elements are considered for pulse shifting. So, the ON-time duration and the switch-ON time instants of all the outer elements within each modulation period are considered for the minimization of SBLs. The cost function (CF) for the overall minimization of SLL and SBLs is expressed as

$$\mathrm{CF} = \mathrm{w}_1 * (\mathrm{SLL}_{\max}^{(i)})\Big|_{\mathrm{f}_0} + \mathrm{w}_2 * (\mathrm{SBL}_{\max}^{(i)})\Big|_{\mathrm{f}_0 + \mathrm{mf}_\mathrm{p}} + \mathrm{FNBW}^{(i)} \tag{13}$$

where i is the number of iterations for the evolutionary optimization; $\mathrm{SLL}_{\max}$ and $\mathrm{SBL}_{\max}$ are the maximum sidelobe level at the fundamental frequency and the maximum sideband level at the harmonic frequencies respectively; FNBW represents the beam width between the first nulls of the radiation pattern of the array; w_1 and w_2 are the real-valued weighting factors to balance the different contributions to the CF. For this minimization problem, equal contributions have been considered for $\mathrm{SLL}_{\max}$ and $\mathrm{SBL}_{\max}$ ($w_1 = w_2 = 1.2$).

III. EVOLUTIONARY OPTIMIZATION EMPLOYED

Evolutionary optimization methods can be designated as population-based meta-heuristic search processes influenced by natural phenomena. Due to the adaptive nature, these stochastic methods are capable of producing a sufficiently good solution to the optimization problem. The musical harmony-based IHSA is employed in this work, and the results obtained from IHSA are compared with the results of other applied algorithms such as HSA, PSO, and RGA. IHSA based results combined with pulse shifting of outer elements outperform HSA, PSO, and RGA based results.

A. IMPROVED HARMONY SEARCH ALGORITHM

Harmony search algorithm (HSA) is based on improvisation of musical harmony, an artificial phenomenon of creating music from a combination of sounds, with aesthetic pleasure. HSA searches for a global solution just as a musician searches for the best combination of random harmonies from different musical instruments to create the most pleasing music. Pitch adjustments for different instruments play a decisive role in this process. In the mathematical modelling of this harmony, four adjustable parameters are used to get the near-global optimum solution. These parameters are harmony memory size (HMS), harmony memory considering rate (HMCR), pitch adjusting rate (PAR), and fret width (FW). PAR and FW dominate the exploitation process by utilizing the gained information to achieve the desired goal. On the other hand, the ability to search uncovered areas or the exploration process is controlled by HMCR. HMCR also behaves as an exploitation agent as the number of iteration increases. The balance between exploitative and explorative capabilities can be achieved with these adjustable parameters to get the optimal solution. A detailed discussion of HSA, introduced by Geem *et al*., can be found in [40].

Improved HSA (IHSA), proposed by Mahdavi *et al*. [41], is an enhanced version of original HSA with dynamic PAR and FW, changing with the number of iterations. The flowchart of IHSA is presented in Fig. 4, and the basic steps of IHSA are illustrated as follows [42]:

Step 1: The parameters of IHSA, such as HMCR, HMS, minimum PAR (PAR_{min}), maximum PAR (PAR_{max}), minimum FW (FW_{min}), maximum FW (FW_{max}), and the number of iterations (NI) will be initialized. The optimization problem will also be determined using a suitable objective function $f(x_i)$, where x_i will be the possible solutions from N (where N $\in$ *number of decision variables of* x_i).

Step 2: Harmony memory (HM) matrix will be generated with as many random solution vectors as HMS, where HMS is the number of rows in the HM matrix, and each column represents the notes played by a musician, can be expressed as

$$HM = \begin{bmatrix} x_1^1 & x_2^1 & \cdots & x_{N-1}^1 & x_N^1 \\ x_1^2 & x_2^2 & \cdots & x_{N-1}^2 & x_N^2 \\ \vdots & \vdots & \cdots & \vdots & \vdots \\ x_1^{HMS-1} & x_2^{HMS-1} & \cdots & x_{N-1}^{HMS-1} & x_N^{HMS-1} \\ x_1^{HMS} & x_2^{HMS} & \cdots & x_{N-1}^{HMS} & x_N^{HMS} \end{bmatrix} \tag{14}$$

HM will be initialized within the lower and upper boundary using the following equation:

$$x_i = LB + r_1 * (\text{UB-LB}) \tag{15}$$

where r_1 is a random number between 0 and 1. LB and UB are the lower bounds and upper bounds of each decision variable such that, $LB \leq x_i \leq UB$.

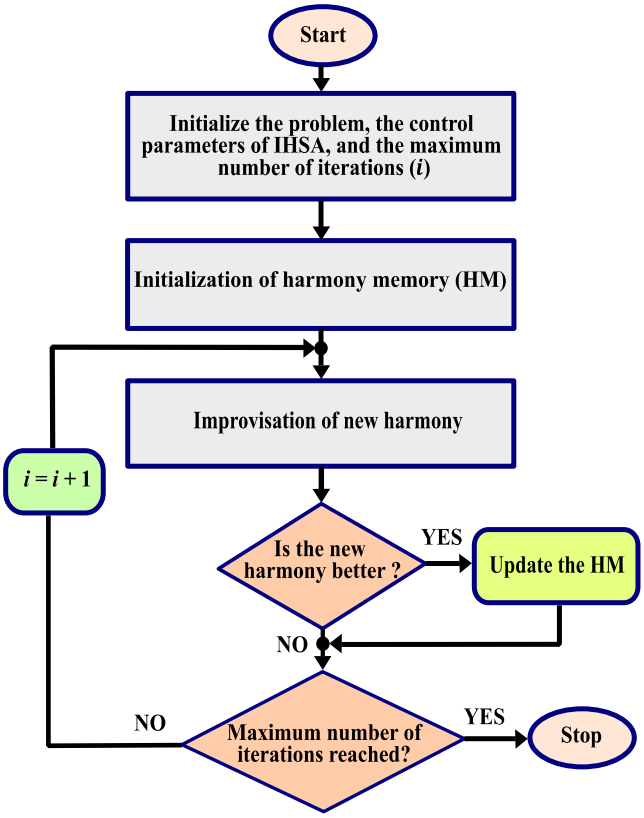

FIGURE 4. Flowchart of IHSA.

Step 3: The new harmony will be generated using a combination of HMCR, PAR, and FW. This process of improvising new harmony has two main steps.

First, two random values (r_2 and r_3) will be created between 0 and 1. If $r_2 >$ HMCR, a new value x_j^{new} will be created using Eq. (15). Otherwise, if $r_2 <$ HMCR, a random value will be selected from HM with a rate of (1 – HMCR), and if $r_3 < PAR(gn)$, the new harmony x_i will be modified using the following equation:

$$x_j^{new} = x_j^{new} \pm r_4 * FW\,(gn) \tag{16}$$

where r_4 is a random number between 0 and 1.

$PAR(gn)$ and $FW(gn)$ are the dynamic values of PAR and FW changing with generation or number of iterations expressed as follows:

$$PAR\,(gn) = PAR_{min} + \frac{PAR_{max} - PAR_{min}}{NI} * gn \tag{17}$$

$$FW\,(gn) = FW_{max} * exp\left\{\frac{ln\left(\frac{FW_{min}}{FW_{max}}\right)}{NI} * gn\right\} \tag{18}$$

Step 4: If the newly generated harmony is better than the worst harmony in the HM, the new harmony will be updated by discarding the worst harmony, based on the objective function.

Step 5: If the maximum number of iterations is reached, the process will be terminated. Otherwise, step 3 and 4 will be repeated until the stopping criteria is satisfied.

The conventional HSA requires more number of iterations to achieve a near-global optimum solution due to the fixed value of PAR and FW [41]. The convergence rate and the fine-tuning of optimal solution vectors depends on the adjustments of these two parameters. Small PAR with large FW can be beneficial in initial generations. The large values of FW contribute to get more diverse solutions and enhance the algorith's exploration process. But, at the same time, it requires more number of iterations to reach the optimal solution. For the final stages of iterations, large PAR with small FW helps the algorithm for better tuning the solution. In IHSA, Mahdavi *et al*. [41] have introduced a method of balancing these two parameters by proposing two new equations presented in Eq. (17) and Eq. (18). Dynamically changing PAR and FW values have enhanced the performance of IHSA over HSA and other opted algorithms.

B. OTHER OPTIMIZATION TECHNIQUES EMPLOYED

Other well-known algorithms, such as PSO and RGA, are also employed with the optimal pulse shifting scheme proposed in this paper. A detailed discussion of these algorithms can be found in [43]–[46]. IHSA based results are compared with the results obtained from other applied algorithms to show a fair comparison between them for this optimization problem. Representative results are reported to prove the superiority of IHSA over other opted algorithms.

IV. RESULTS AND DISCUSSION

This section deals with the numerical results and the detailed analysis of the proposed approach, where evolutionary algorithms and pulse shifting strategies are used to achieve ultra-low SLL and SBL for TMLA. Numerical results for two sets of array structures with 16 and 30 isotropic elements are presented here using MATLAB. IHSA, HSA, PSO, and RGA are employed with best-proven control parameters to optimize the proposed scheme of switching as well as excitation coefficients of the array elements. Outcomes of these algorithms for two sets of arrays are reported. The best results obtained by IHSA are compared with already published literature results for the simultaneous reduction of SLL and SBL. All computations are performed on Intel(R) Core (TM) i5-8250U CPU @ 1.80 GHz with 8 GB RAM. The best-proven control parameters for all the algorithms are selected after several runs, presented in Table 1.

Considering uniformly excited ($I_n = 1$) linear array with 0.5λ equally spaced isotropic elements and uniform normalized ON-time duration (i.e., all the elements are ON), the non-optimized values of SLL, FNBW, and directivity are calculated. For the 16-element and the 30-element array, the values of SLL, FNBW, and directivity are −13.15 dB, 14.4°, 12.04 dB, and −13.24 dB, 7.56°, 14.77 dB, respectively.

TABLE 1. Control parameters of RGA, PSO, HSA, and IHSA.

Algorithm	Parameters	Values
RGA	Population size	120
	Iteration cycles	300
	Mutation rate	0.01
	Crossover rate	0.8
	Selection probability	1/3
PSO	Population size	120
	Iteration cycles	300
	Inertia weight	0.5
	Cognitive acceleration constant (C_1)	2.05
	Social acceleration constant (C_2)	2.05
HSA	Harmony memory size (HMS)	100
	Harmony memory considering rate (HMCR)	0.95
	Pitch adjustment rate (PAR)	0.35
	Fret width (FW)	0.02
	Iteration cycles	300
IHSA	HMS	100
	HMCR	0.95
	Minimum PAR	0.35
	Maximum PAR	0.9
	Minimum FW	0.00002
	Maximum FW	0.02
	Iteration cycles	300

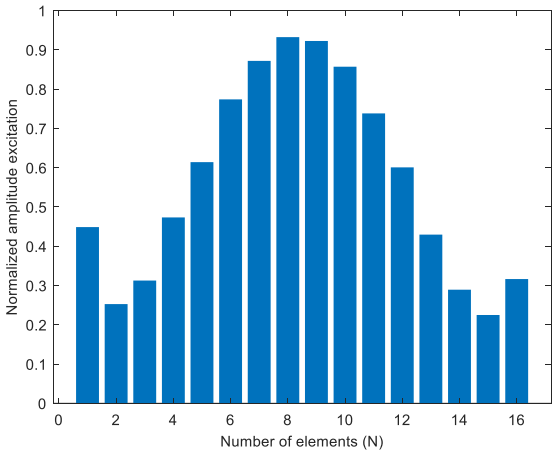

FIGURE 5. Normalized amplitude excitations for 16-element TMLA.

A. 16-ELEMENT TMLA

For the 16-element TMLA, the optimized excitation amplitudes and the switching sequence using IHSA are presented in Fig. 5 and Fig. 6. The ON-time duration of four outer elements (element number 1, 2, and 15, 16) are considered for optimization as well as pulse shifting to reduce the SBL so that the undesired radiation in sidebands can be spread over the whole angle of arrival region as uniformly as possible. For

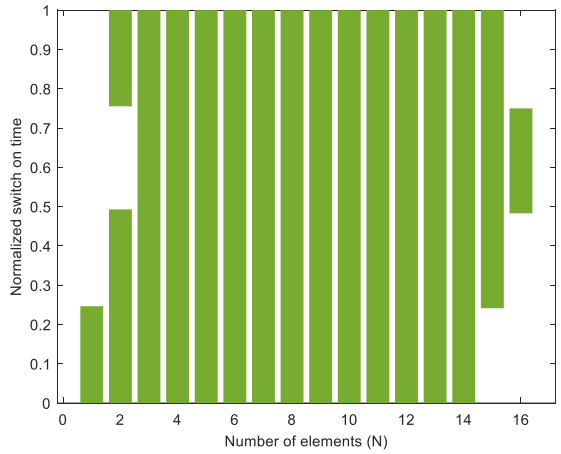

FIGURE 6. Normalized switch-ON sequence for 16-element TMLA.

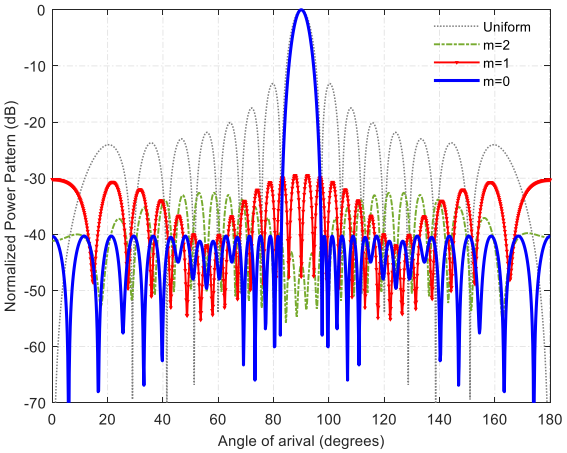

FIGURE 7. Radiation patterns for 16-element TMLA with IHSA based approach and pulse shifting.

the rest of the elements (element number 3 to 14), uniform ON-time durations ($\tau_n = 1$) are considered. The optimized excitations (I_n) of Fig. 5 and the pulse-shifted sequence of Fig. 6, along with the optimized inter-element spacing of 0.8886λ, are considered for the simultaneous reduction of SLL and SBL. The radiation patterns for 16-element TMLA at the fundamental frequency (f_0 at $m = 0$), as well as harmonic frequencies ($f_0 + mf_p$, at $m = 1, 2$), are presented in Fig. 7.

The IHSA based approach has achieved an ultra-low SLL_{max} of −40.31 dB in comparison to −13.15 dB SLL_{max} of the uniform pattern. The SLL_{max} obtained from HSA, PSO, and RGA based approaches are −37.31 dB, −37.86 dB, and −33.86 dB, respectively. The reduced values of SBLs for the first two positive harmonics with IHSA based optimized and shifted pulses at the outer elements of the array are presented as $\text{SBL}^1_{\text{max}} = -29.47$ dB and $\text{SBL}^2_{\text{max}} = -32.59$ dB. The first two positive SBLs without optimized and pulse-shifted switching sequences are reported as $\text{SBL}^1_{\text{max}} = -11.25$ dB and $\text{SBL}^2_{\text{max}} = -15.76$ dB. So, the proposed approach's effectiveness with pulse shifting

TABLE 2. Results obtained for 16-element TMLA with applied algorithms.

Algorithm	SLL_{max} (dB)	SBL^1_{max} (dB)	SBL^2_{max} (dB)	FNBW ($degree$)	Directivity (dB)
IHSA	**-40.31**	**-29.47**	**-32.59**	**15.12**	**13.2947**
HSA	-37.31	-28.24	-31.39	14.76	13.2269
PSO	-37.86	-28.15	-31.16	14.78	13.2422
RGA	-33.86	-26.71	-29.73	13.68	13.3794

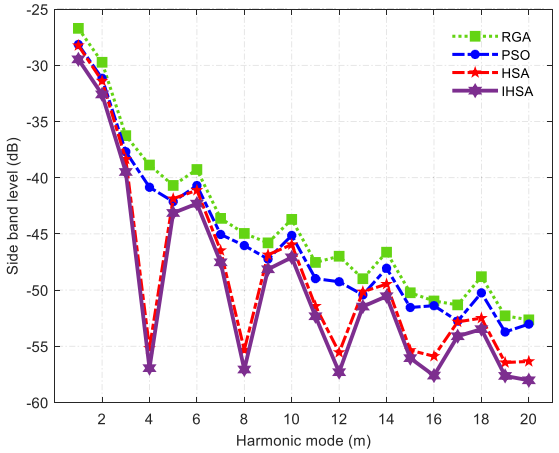

FIGURE 8. First 20 positive SBLs for IHSA, HSA, PSO, and RGA based approach for 16-element TMLA.

is clearly visible in terms of the first two SBLs with a reduction of 18.22 dB and 16.83 dB. The SLL is also lowered by 27.16 dB from the uniform pattern. The $\text{SBL}^1_{\text{max}}$ obtained from HSA, PSO, and RGA based approaches are −28.24 dB, −28.15 dB, and −26.71 dB. The $\text{SBL}^2_{\text{max}}$ with these algorithms are reported as −31.39 dB, −31.16 dB, and −29.73 dB. Thus, IHSA based results outperform HSA, PSO, and RGA based results in terms of reduced SLL and SBL. The FNBW and the directivity reported for IHSA are 15.12° and 13.2947 dB in comparison to 14.4° and 12.04 dB of the uniform pattern. Numerical results obtained from IHSA, HSA, PSO, and RGA based approaches are presented in Table 2.

SBLs obtained at first twenty positive harmonics using IHSA, HSA, PSO, and RGA are shown in Fig. 8, which confirms that the proposed approach reduces all other SBLs below the level of $\text{SBL}^1_{\text{max}}$. A comparison of SBLs at first two positive harmonics is shown in Fig. 9 when the number of outer elements considered for pulse shifting increases. Shifting of pulses results in gain reduction. For a 16-element TMLA, the estimated reduction in gain with an increasing number of pulse-shifted elements is also presented in Fig. 9. From the figure, it is clear that the reduction in gain is always positive, which implies that the pattern with pulse-shifted elements has a lesser gain than the pattern without pulse shift. The reduction in gain and SBLs also decrease when the number of outer elements considered for pulse shifting decreases. For example, reduction in gain and the first two positive SBLs by controlling 4 and 6 outer elements

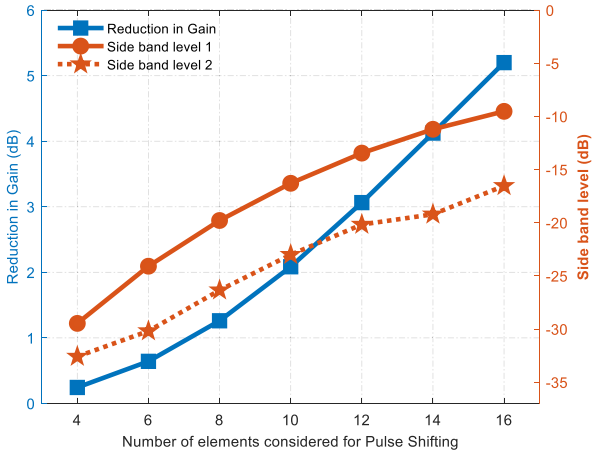

FIGURE 9. Comparisons of SBL1, SBL2, and reduction in gain with different number of elements considered for pulse shifting with IHSA (N = 16).

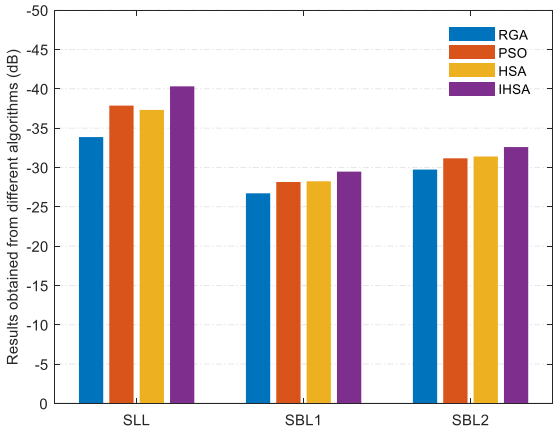

FIGURE 10. Comparison of IHSA, HSA, PSO, and RGA based results in terms of SLL, SBL1, and SBL2 for 16-element TMLA.

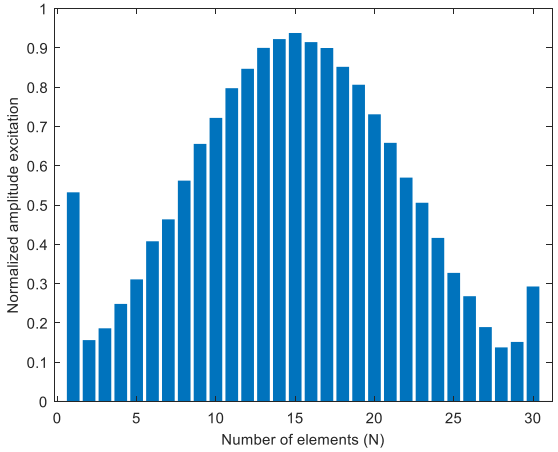

FIGURE 11. Normalized amplitude excitations for 30-element TMLA.

are reported as 0.2434 dB, −29.47 dB, −32.59 dB, and 0.6420 dB, −24.09 dB, −30.19 dB, respectively. Fig. 9 also shows that a reduction in gain of less than 1 dB can be achieved when the number of outer elements considered for pulse shifting is not more than 6. So, the best results in terms of SBLs are obtained by controlling four outer elements with a gain reduction of only 0.2434 dB for 16-element TMLA.

The best results obtained by the IHSA based approach for the 16-element TMLA is also compared with previously published results. The SLL and SBL with optimized time sequences and uniform amplitude excitation are reported as −25.5 dB and −24.6 dB using a genetic algorithm (GA) in [9]. Considering a static Chebyshev excitation of −30 dB, pulse shifting is applied with PSO for the reduction of the SBL^1_{max} and SBL^2_{max} up to −19.5 dB and −21.7 dB in [24]. Phase modulation-based approach with −20.21 dB, −19.28 dB of SBL^1_{max} and −22.33 dB, −20.79 dB of SBL^2_{max} have been reported with two different examples in [47]. SBL of −21.12 dB with −30 dB SLL is presented for beam scanning purpose in [48]. Pulse splitting and shifting with static amplitude excitation has improved the SBL to −22.51 dB while maintaining a −30 dB SLL at the fundamental pattern, shown in [26]. Further improvement in SBL has been reported as −27.8 dB with sub-sectional switching sequences optimized with differential evolution (DE) algorithm [25].

The proposed approach with IHSA and pulse shifting to the outer elements outperform the already published best result with a reduction of 10.31 dB in SLL. The first two positive SBLs for the 16-element TMLA is also improved to −29.47 dB and −32.59 dB from the already reported best results of −27.8 dB and −22.33 dB, respectively. The proposed approach of controlling outer elements is also implemented with HSA, PSO, and RGA. The results obtained by these algorithms are compared with IHSA based results to show the superior performance of IHSA over others, presented in Fig. 10.

B. 30-ELEMENT TMLA

For the 30-element TMLA, the optimized excitation amplitudes using IHSA are presented in Fig. 11. The optimized ON-time sequences with four number of outer elements (element number 1, 2, and 29, 30) considered for pulse shifting are presented in Fig. 12. For the rest of the elements (element number 3 to 28), uniform ON-time durations ($\tau_n = 1$) are considered. The optimized excitations (I_n) of Fig. 11 and the pulse-shifted sequence of Fig. 12, along with the optimized inter-element spacing of 0.9096λ, are considered for the simultaneous reduction of SLL and SBL. The radiation patterns for 30-element TMLA at the fundamental frequency (f_0 at $m = 0$), as well as harmonic frequencies ($f_0 + mf_p$, at $m = 1, 2$), are presented in Fig. 13.

The IHSA based approach has achieved an ultra-low SLL_{max} of −41.15 dB in comparison to −13.24 dB SLL_{max} of the uniform pattern. The SLL_{max} obtained from HSA, PSO, and RGA based approaches are −37.49 dB, −30.17 dB, and −25.88 dB, respectively. The reduced values of SBLs for the first two positive harmonics with IHSA based optimized and shifted pulses at the outer elements of the array are

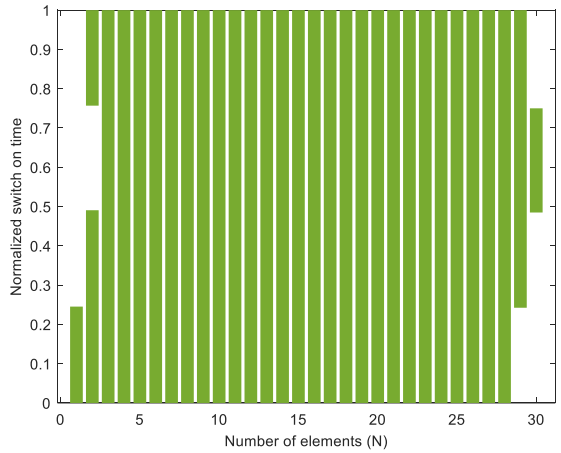

FIGURE 12. Normalized switch-ON sequence for 30-element TMLA.

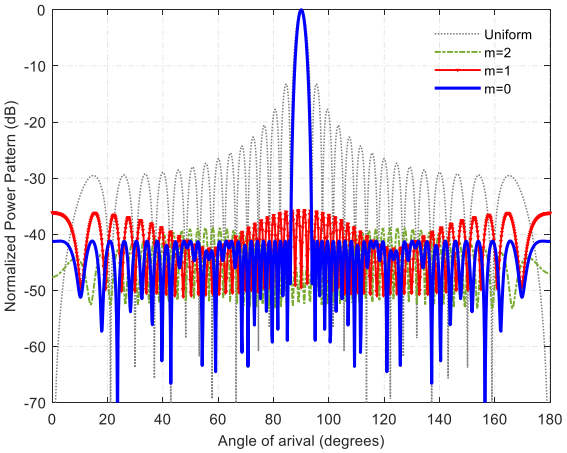

FIGURE 13. Radiation patterns for 30-element TMLA with IHSA based approach and pulse shifting.

presented as $\text{SBL}^1_{\text{max}} = -35.71$ dB and $\text{SBL}^2_{\text{max}} = -38.82$ dB. The first two positive SBLs without optimized and pulse-shifted switching sequences are reported as $\text{SBL}^1_{\text{max}} = -11.15$ dB and $\text{SBL}^2_{\text{max}} = -15.64$ dB. Due to the flexibility of the proposed approach, the SBLs at the first two positive harmonics show a reduction of 24.56 dB and 23.18 dB. The SLL is also lowered by 27.91 dB from the uniform pattern. The $\text{SBL}^1_{\text{max}}$ obtained with HSA, PSO, and RGA based approaches are −34.13 dB, −30.38 dB, and −29.39 dB. The $\text{SBL}^2_{\text{max}}$ with these algorithms are reported as −37.45 dB, −33.39 dB, and −32.4 dB. Thus, IHSA outperforms HSA, PSO, and RGA in terms of reduced SLL and SBL. The FNBW and the directivity reported for IHSA are 7.92° and 16.1579 dB in comparison to 7.56° and 14.77 dB of the uniform pattern, respectively. Numerical results obtained from IHSA, HSA, PSO, and RGA based approaches are presented in Table 3.

SBLs obtained at first twenty positive harmonics using IHSA, HSA, PSO, and RGA are shown in Fig. 14, which implies that the proposed approach reduces all other SBLs below the level of $\text{SBL}^1_{\text{max}}$. The estimation of reduction in gain and nature of SBLs with an increasing number of

TABLE 3. Results obtained for 30-element TMLA with applied algorithms.

Algorithm	SLL_{max} (dB)	SBL^1_{max} (dB)	SBL^2_{max} (dB)	FNBW $(degree)$	Directivity (dB)
IHSA	**-41.15**	**-35.71**	**-38.82**	**7.92**	**16.1579**
HSA	-37.49	-34.13	-37.45	7.20	16.3599
PSO	-30.17	-30.38	-33.39	8.28	15.4967
RGA	-25.88	-29.39	-32.4	5.76	16.6436

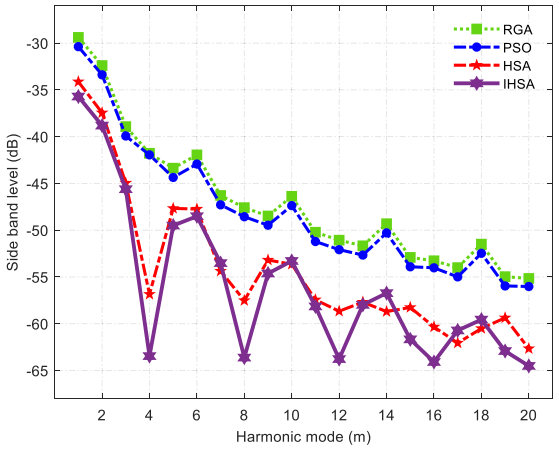

FIGURE 14. First 20 positive SBLs for IHSA, HSA, PSO, and RGA based approach for 30-element TMLA.

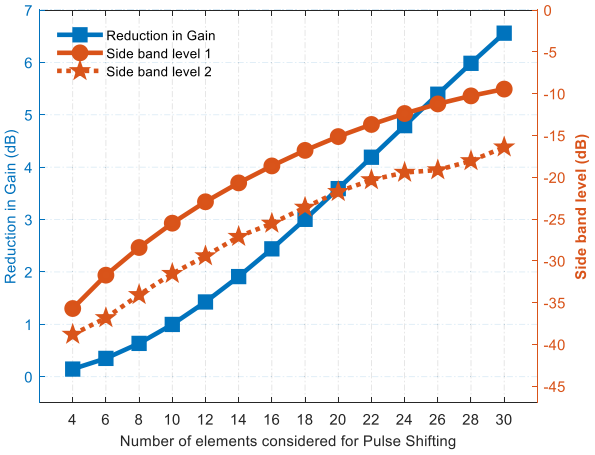

FIGURE 15. Comparisons of SBL1, SBL2, and reduction in gain with different number of elements considered for pulse shifting with IHSA (N = 30).

pulse-shifted elements for the IHSA based approach is presented in Fig. 15. For a 30-element TMLA, less than 1 dB reduction in gain can be achieved when the number of outer elements considered for pulse shifting is not more than 10. The reduction in gain by controlling 4, 6, 8, and 10 number of outer elements are reported as 0.1457 dB, 0.3494 dB, 0.6358 dB, and 0.9976 dB, respectively. So, the best results in terms of SBLs are obtained by controlling four outer elements

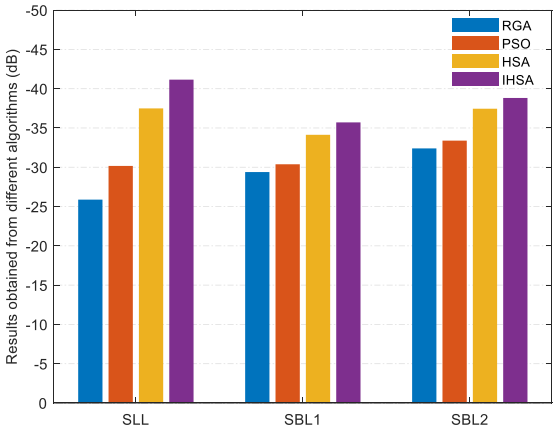

FIGURE 16. Comparison of IHSA, HSA, PSO, and RGA based results in terms of SLL, SBL1, and SBL2 for 30-element TMLA.

with a gain reduction of only 0.1457 dB for 30-element TMLA.

The best results obtained for 30-element TMLA with IHSA are compared with already published literature results. The SLL and SBL of −20.04 dB and −30.08 dB with optimized time sequences through simulated annealing (SA) is reported in [8]. PSO based pulse shifting strategy is implemented for the reduction of SBL to −28.9 dB and −32.90 dB in [23] and [24]. Further reduction in SBL is performed with DE based array thinning approach, and −34.08 dB of SBL along with −23.01 dB of SLL is reported in [22]. Further improvement with −28 dB SLL along with −30 dB of SBL has been published in [49] for pencil beam pattern generated with 30-element TMLA.

The proposed approach with IHSA and pulse shifting to the outer elements outperform the already published best result with a reduction of 13.15 dB in SLL. The reduced SBLs for the 30-element linear TMAA is reported as −35.71 dB and −38.82 dB with considerable improvement over −34.08 dB and −35.10 dB of the previously published best result. The previously reported best FNBW of 9.34° [8] is also improved to a narrower FNBW of 7.92° along with a simultaneous reduction in SLL and SBL with the proposed approach. The proposed approach of controlling outer elements is also implemented with HSA, PSO, and RGA. The results obtained by these algorithms are compared with IHSA based results to show the superior performance of IHSA over other algorithms and presented in Fig. 16.

To illustrate the effectiveness of the proposed approach, the best results obtained for 16- and 30- element TMLAs are compared with already published works and presented in Table 4. The proposed IHSA based approach outperforms other results in terms of SLL, SBLs, FNBW, and directivity.

C. COMPARISONS OF ACCURACY

To find the accuracy and stability of the best performing algorithm, Two-sample t-test with an equal sample size of 10 $n_a = n_b$, where n_a and n_b are the sample sizes of the first and second algorithm) is performed at the default 5% significance level $\alpha = 0.05$). Two sample t-test is a hypothesis testing method for determining the statistically significant difference between two independent samples of equal sample size [50]. The positive values of the t-test imply that the first algorithm is performing better than the other one. The p-values are calculated using students' t cumulative distribution function [50]. If the p-value is less than the significance level (α), the null hypothesis can be rejected with $100(1-\alpha)$ % confidence level which implies that the proposed algorithm can be accepted with 95% confidence over the other algorithm if the default value of significance level $\alpha = 0.05$) is considered. The critical values of the t-test for comparing two independent samples for different values of α and v (v is the degree of freedom $= min\{n_a - 1, n_b - 1\}$) are given in [50]. The t-test values and p-values of IHSA over HSA, PSO, and RGA for 16-element TMLA results are presented in Table 5. If the t-test values are higher than 2.821, 2.998,

TABLE 4. Comparison of the proposed approach with already published literature results in terms of SLL, SBLs, and directivity.

Element No.	Reference Paper	SLL_{max} (dB)	SBL^1_{max} (dB)	SBL^2_{max} (dB)	Directivity (dB)
16	Ref. [9]	-25.50	-24.60	*NR	*NR
	Ref. [24]	-30.00	-19.50	-21.70	*NR
	Ref. [26]	-30.00	-22.51	*NR	*NR
	Ref. [25]	-30.00	-27.80	*NR	*NR
	Ref. [47] Example 1	-30.00	-20.21	-22.33	*NR
	Ref. [47] Example 2	-30.00	-19.28	-20.79	*NR
	Ref. [48]	-30.00	-21.12	*NR	*NR
	Proposed	**-40.31**	**-29.47**	**-32.59**	**13.2947**
30	Ref. [8]	-20.04	-30.08	*NR	*NR
	Ref. [24]	-20.04	-32.90	*NR	*NR
	Ref. [23]	-20.00	-28.90	-35.10	14.94
	Ref. [22] Example 1	-23.01	-34.08	*NR	*NR
	Ref. [22] Example 2	-21.84	-33.77	*NR	*NR
	Ref. [49]	-28.00	-30.00	*NR	*NR
	Proposed	**-41.15**	**-35.71**	**-38.82**	**16.1579**

TABLE 5. t-test values and p-values for comparison of IHSA with other applied algorithms for 16-element TMLA.

Algorithms	t-test value	p-value
IHSA/HSA	8.299813389409204	8.239039165247597e-06
IHSA/PSO	9.927744337276877	1.900375465324622e-06
IHSA/RGA	12.603552277689712	2.531940620498219e-07

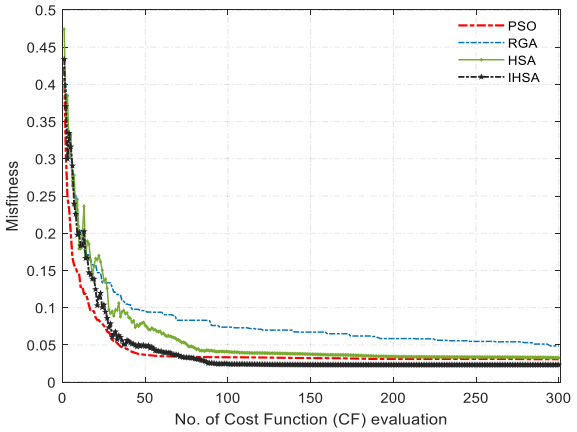

FIGURE 17. Convergence profiles of proposed algorithms for 16-element TMLA.

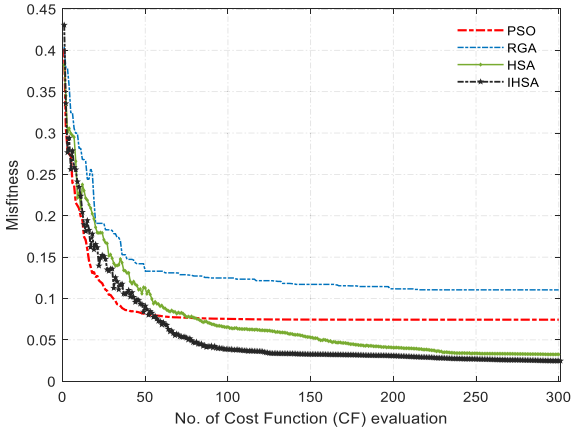

FIGURE 18. Convergence profiles of proposed algorithms for 30-element TMLA.

3.250, 3.690, 4.781 (for $v = 9$), then there is a significant difference between the two algorithms with 99%, 99.25%, 99.5%, 99.75%, 99.95% confidence levels, respectively [50]. The t-test values presented in Table 5 implies that all the values are greater than the threshold value of 4.781 for 99.95% confidence level. The p-values obtained for this comparison are also much lesser than 0.05. So, IHSA is a significantly better performing algorithm over the other applied algorithms for this particular problem with more than 99.95% confidence level.

V. CONVERGENCE PROFILES

The evolutionary algorithms are compared in terms of cost function (CF) values. The minimum cost values of each algorithm against the total number of iterations performed are recorded for the convergence profile. Convergence profiles for TMLAs with 16 and 30 elements are presented in Fig. 17 and Fig. 18, respectively.

IHSA based profiles for both sets of antenna arrays have converged to optimal lowest fitness values in comparison to HSA, PSO, and RGA. Thus, the performance of IHSA can be considered as the best among the applied algorithms for this particular design problem.

VI. CONCLUSION

In this paper, a simultaneous reduction of sidelobe level (SLL) and sideband levels (SBLs) of time-modulated linear arrays (TMLAs) are presented with optimized excitation and switching sequences. The outer elements of the array are controlled with pulse shifting to reduce the SBL while maintaining an ultra-low SLL at the fundamental pattern in an IHSA based approach. The proposed approach also outperforms HSA, PSO, and RGA based results towards achieving the desired goal. The ultra-low SLLs obtained for 16- and 30-element TMLAs are reported as −40.31 dB and −41.15 dB, which implies a considerable improvement compared to the already published best results. The first two positive SBLs for 16- and 30-element TMLAs with −29.47 dB, −32.59 dB, and −35.71 dB, −38.82 dB has shown the effectiveness of the proposed approach compared to the already published methods of sideband reduction. The proposed method also maintains a narrow FNBW, which implies a highly directive main beam at the fundamental pattern. Directivity maximization is also considered as one of the important aspects of this optimization problem. For both sets of TMLAs, the optimized pattern's directivity has improved over the uniform pattern. For all the cases, fully filled or illuminated arrays are considered, so that all the elements can contribute to generating the desired pattern according to the optimized values. Here, the switching sequences of outer elements are optimized, and uniform switching sequences are considered for the rest of the elements. So, the number of switches required is lesser than the total number of elements present in the array, which, in turn, reduces the complexity of the switching network. Thus, the proposed approach is suitable for achieving multiple objectives such as SLL reduction, SBL reduction, FNBW improvement, and directivity maximization, simultaneously.

REFERENCES

[1] R. L. Haupt, "Antenna array basics," *Antenna Arrays*, pp. 1–44, 2010.
[2] H. Schrank, "Low sidelobe phased array antennas," *IEEE Antennas Propag. Soc. Newslett.*, vol. 25, no. 2, pp. 4–9, Apr. 1983, doi: 10.1109/MAP.1983.27670.
[3] H. E. Shanks and R. W. Bickmore, "Four-dimensional electromagnetic radiators," *Can. J. Phys.*, vol. 37, no. 3, pp. 263–275, Mar. 1959, doi: 10.1139/p59-031.
[4] W. Kummer, A. Villeneuve, T. Fong, and F. Terrio, "Ultra-low sidelobes from time-modulated arrays," *IEEE Trans. Antennas Propag.*, vol. 11, no. 6, pp. 633–639, Nov. 1963, doi: 10.1109/TAP.1963.1138102.
[5] H. Shanks, "A new technique for electronic scanning," *IRE Trans. Antennas Propag.*, vol. 9, no. 2, pp. 162–166, Mar. 1961, doi: 10.1109/TAP.1961.1144965.
[6] S. Yang, Y. Beng Gan, and A. Qing, "Sideband suppression in time-modulated linear arrays by the differential evolution algorithm," *IEEE Antennas Wireless Propag. Lett.*, vol. 1, pp. 173–175, 2002, doi: 10.1109/LAWP.2002.807789.
[7] S. Yang, Y. B. Gan, and P. K. Tan, "Comparative study of low sidelobe time modulated linear arrays with different time schemes," *J. Electromagn. Waves Appl.*, vol. 18, no. 11, pp. 1443–1458, Jan. 2004, doi: 10.1163/1569393042954910.

[8] Fondevila, Bregains, Ares, and Moreno, "Optimizing uniformly excited linear arrays through time modulation," *IEEE Antennas Wireless Propag. Lett.*, vol. 3, pp. 298–301, 2004, doi: 10.1109/LAWP.2004.838833.

[9] S. Yang, Ye, A. Qing, and P. Khiang Tan, "Design of a uniform amplitude time modulated linear array with optimized time sequences," *IEEE Trans. Antennas Propag.*, vol. 53, no. 7, pp. 2337–2339, Jul. 2005, doi: 10.1109/TAP.2005.850765.

[10] J. Fondevila, J. C. Brégains, F. Ares, and E. Moreno, "Application of time modulation in the synthesis of sum and difference patterns by using linear arrays," *Microw. Opt. Technol. Lett.*, vol. 48, no. 5, pp. 829–832, May 2006, doi: 10.1002/mop.21489.

[11] G. Li, S. Yang, M. Huang, and Z. Nie, "Shaped patterns synthesis in time-modulated antenna arrays with static uniform amplitude and phase excitations," *Frontiers Electr. Electron. Eng. China*, vol. 5, no. 2, pp. 179–184, Jun. 2010, doi: 10.1007/s11460-010-0005-2.

[12] G. Li, S. Yang, and Z. Nie, "A study on the application of time modulated antenna arrays to airborne pulsed Doppler radar," *IEEE Trans. Antennas Propag.*, vol. 57, no. 5, pp. 1578–1582, May 2009, doi: 10.1109/TAP.2009.2016788.

[13] A. Tennant, "Experimental two-element time-modulated direction finding array," *IEEE Trans. Antennas Propag.*, vol. 58, no. 3, pp. 986–988, Mar. 2010, doi: 10.1109/TAP.2009.2039301.

[14] G. Li, S. Yang, and Z. Nie, "Direction of arrival estimation in time modulated linear arrays with unidirectional phase center motion," *IEEE Trans. Antennas Propag.*, vol. 58, no. 4, pp. 1105–1111, Apr. 2010, doi: 10.1109/TAP.2010.2041313.

[15] G. Li, S. Yang, Y. Chen, and Z. Nie, "A novel electronic beam steering technique in time modulated antenna arrays," *Prog. Electromagn. Res.*, vol. 97, pp. 391–405, 2009, doi: 10.2528/PIER09072602.

[16] Y. Tong and A. Tennant, "Simultaneous control of sidelobe level and harmonic beam steering in time-modulated linear arrays," *Electron. Lett.*, vol. 46, no. 3, pp. 200–202, 2010, doi: 10.1049/el.2010.2629.

[17] L. Poli, P. Rocca, G. Oliveri, and A. Massa, "Harmonic beamforming in time-modulated linear arrays," *IEEE Trans. Antennas Propag.*, vol. 59, no. 7, pp. 2538–2545, Jul. 2011, doi: 10.1109/TAP.2011.2152323.

[18] G. Ram, D. Mandal, R. Kar, and S. P. Ghoshal, "Directivity maximization and optimal far-field pattern of time modulated linear antenna arrays using evolutionary algorithms," *AEU-Int. J. Electron. Commun.*, vol. 69, no. 12, pp. 1800–1809, Dec. 2015, doi: 10.1016/j.aeue.2015.09.009.

[19] G. Ram, D. Mandal, M. A. Panduro, R. Kar, and Z. Raida, "Optimal design of timed antenna arrays for SLL reduction, dual and multiple broad nulls in the radiation pattern," *IETE Tech. Rev.*, to be published, doi: 10.1080/02564602.2019.1699453.

[20] K. Guney and S. Basbug, "Null synthesis of time-modulated circular antenna arrays using an improved differential evolution algorithm," *IEEE Antennas Wireless Propag. Lett.*, vol. 12, pp. 817–820, 2013, doi: 10.1109/lawp.2013.2271273.

[21] G. Li, S. Yang, M. Huang, and Z. Nie, "Sidelobe suppression in time modulated linear arrays with unequal element spacing," *J. Electromagn. Waves Appl.*, vol. 24, nos. 5–6, pp. 775–783, Jan. 2010, doi: 10.1163/156939310791036368.

[22] E. Aksoy and E. Afacan, "Thinned nonuniform amplitude time-modulated linear arrays," *IEEE Antennas Wireless Propag. Lett.*, vol. 9, pp. 514–517, 2010, doi: 10.1109/LAWP.2010.2051312.

[23] L. Poli, P. Rocca, L. Manica, and A. Massa, "Handling sideband radiations in time-modulated arrays through particle swarm optimization," *IEEE Trans. Antennas Propag.*, vol. 58, no. 4, pp. 1408–1411, Apr. 2010, doi: 10.1109/TAP.2010.2041165.

[24] L. Poli, P. Rocca, L. Manica, and A. Massa, "Pattern synthesis in time-modulated linear arrays through pulse shifting," *IET Microw., Antennas Propag.*, vol. 4, no. 9, pp. 1157–1164, 2010, doi: 10.1049/iet-map.2009.0042.

[25] Q. Zhu, S. Yang, L. Zheng, and Z. Nie, "Design of a low sidelobe time modulated linear array with uniform amplitude and sub-sectional optimized time steps," *IEEE Trans. Antennas Propag.*, vol. 60, no. 9, pp. 4436–4439, Sep. 2012, doi: 10.1109/TAP.2012.2207082.

[26] E. Aksoy and E. Afacan, "Sideband level suppression improvement via splitting pulses in time modulated arrays under static fundamental radiation," in *Proc. Prog. Electromagn. Res. Symp.*, no. 2, 2011, pp. 364–367.

[27] E. Aksoy and E. Afacan, "An inequality for the calculation of relative maximum sideband level in time-modulated linear and planar arrays," *IEEE Trans. Antennas Propag.*, vol. 62, no. 6, pp. 3392–3397, Jun. 2014, doi: 10.1109/TAP.2014.2311470.

[28] L. Poli, P. Rocca, and A. Massa, "Sideband radiation reduction exploiting pattern multiplication in directive time-modulated linear arrays," *IET Microw., Antennas Propag.*, vol. 6, no. 2, pp. 214–222, Jan. 2012, doi: 10.1049/iet-map.2011.0159.

[29] E. Aksoy and E. Afacan, "A comparative study on sideband optimization in time-modulated arrays," *Int. J. Antennas Propag.*, vol. 2014, pp. 1–14, Apr. 2014, doi: 10.1155/2014/290737.

[30] R. Salgotra and U. Singh, "The naked mole-rat algorithm," *Neural Comput. Appl.*, vol. 31, no. 12, pp. 8837–8857, Dec. 2019, doi: 10.1007/s00521-019-04464-7.

[31] R. Salgotra, U. Singh, and S. Saha, *On Some Improved Versions of Whale Optimization Algorithm*, vol. 44, no. 11. Berlin, Germany: Springer, 2019.

[32] U. Singh, R. Salgotra, and M. Rattan, "A novel binary spider monkey optimization algorithm for thinning of concentric circular antenna arrays," *IETE J. Res.*, vol. 62, no. 6, pp. 736–744, Nov. 2016, doi: 10.1080/03772063.2015.1135086.

[33] U. Singh and R. Salgotra, "Optimal synthesis of linear antenna arrays using modified spider monkey optimization," *Arabian J. Sci. Eng.*, vol. 41, no. 8, pp. 2957–2973, Aug. 2016, doi: 10.1007/s13369-016-2053-2.

[34] R. Salgotra and U. Singh, "A novel bat flower pollination algorithm for synthesis of linear antenna arrays," *Neural Comput. Appl.*, vol. 30, no. 7, pp. 2269–2282, Oct. 2018, doi: 10.1007/s00521-016-2833-3.

[35] U. Singh and R. Salgotra, "Synthesis of linear antenna array using flower pollination algorithm," *Neural Comput. Appl.*, vol. 29, no. 2, pp. 435–445, Jan. 2018, doi: 10.1007/s00521-016-2457-7.

[36] U. Singh and R. Salgotra, "Pattern synthesis of linear antenna arrays using enhanced flower pollination algorithm," *Int. J. Antennas Propag.*, vol. 2017, pp. 1–11, Feb. 2017, doi: 10.1155/2017/7158752.

[37] U. Singh and R. Salgotra, "Synthesis of linear antenna arrays using enhanced firefly algorithm," *Arabian J. for Sci. Eng.*, vol. 44, no. 3, pp. 1961–1976, Mar. 2019, doi: 10.1007/s13369-018-3214-2.

[38] R. Salgotra, U. Singh, S. Saha, and A. K. Nagar, "Improved flower pollination algorithm for linear antenna design problems," in *Proc. Adv. Intell. Syst. Comput.*, 2020, pp. 79–98, doi: 10.1007/978-981-15-0035-0_7.

[39] S. Yang, Y. B. Gan, and P. K. Tan, "Evaluation of directivity and gain for time-modulated linear antenna arrays," *Microw. Opt. Technol. Lett.*, vol. 42, no. 2, pp. 167–171, Jul. 2004, doi: 10.1002/mop.20241.

[40] Z. Woo Geem, J. Hoon Kim, and G. V. Loganathan, "A new heuristic optimization algorithm: Harmony search," *Simulation*, vol. 76, no. 2, pp. 60–68, Feb. 2001, doi: 10.1177/003754970107600201.

[41] M. Mahdavi, M. Fesanghary, and E. Damangir, "An improved harmony search algorithm for solving optimization problems," *Appl. Math. Comput.*, vol. 188, no. 2, pp. 1567–1579, May 2007, doi: 10.1016/j.amc.2006.11.033.

[42] A. A. Al-Omoush, A. A. Alsewari, H. S. Alamri, and K. Z. Zamli, "Comprehensive review of the development of the harmony search algorithm and its applications," *IEEE Access*, vol. 7, pp. 14233–14245, 2019, doi: 10.1109/ACCESS.2019.2893662.

[43] J. Kennedy and R. Eberhart, "Particle swarm optimization," in *Proc. Int. Conf. Neural Netw. (ICNN)*, 1995, vol. 4, no. 6, pp. 1942–1948, doi: 10.1109/ICNN.1995.488968.

[44] Y. Shi and R. Eberhart, "A modified particle swarm optimizer," in *Proc. IEEE Int. Conf. Evol. Comput., IEEE World Congr. Comput. Intell.*, May 2007, pp. 69–73, doi: 10.1109/ICEC.1998.699146.

[45] R. L. Haupt and D. H. Werner, "Anatomy of a genetic algorithm," in *Genetic Algorithms in Electromagnetics* Hoboken, NJ, USA: Wiley, 2007, pp. 29–43.

[46] D. E. Goldberg, *Genetic Algorithms in Search, Optimization, and Machine Learning*. Reading, MA, USA: Addison-Wesley, 1989.

[47] J. Yang, W. Li, and X. Shi, "Phase modulation technique for four-dimensional arrays," *IEEE Antennas Wireless Propag. Lett.*, vol. 13, pp. 1393–1396, 2014, doi: 10.1109/LAWP.2014.2339894.

[48] G. Ni, C. He, J. Chen, Y. Liu, and R. Jin, "Low sideband radiation beam scanning at carrier frequency for time-modulated array by non-uniform period modulation," *IEEE Trans. Antennas Propag.*, vol. 68, no. 5, pp. 3695–3704, May 2020, doi: 10.1109/TAP.2020.2969889.

[49] F. Yang, S. Yang, Y. Chen, and J. Guo, "An effective hybrid approach for the synthesis of pencil beams and shaped beams through 4D linear antenna arrays with constrained DRR," *J. Electromagn. Waves Appl.*, vol. 33, no. 5, pp. 584–600, Mar. 2019, doi: 10.1080/09205071.2018.1564704.

[50] R. E. Walpole, R. H. Myers, S. L. Myers, and K. Ye, *Probability & Statistics for Engineers Scientists*. 2007.

AVISHEK CHAKRABORTY (Graduate Student Member, IEEE) received the B.Tech. degree in electronics and communication engineering and the M.Tech. degree in radiophysics and electronics with a specialization in space science and microwaves from the University of Calcutta, Kolkata, India, in 2017. He is currently pursuing the Ph.D. degree with the Department of Electronics and Communication Engineering, National Institute of Technology (NIT), Durgapur, India, as a full-time Research Scholar. He is also working as a Project Fellow of a DST-SERB funded project with the NIT. His current research interests include antenna array synthesis, the applications of soft computing in antenna array optimization, and radar signal processing.

GOPI RAM received the B.E. degree in electronics and telecommunication engineering from Government Engineering College, Jagdalpur, India, in 2007, and the M.Tech. and Ph.D. degrees from the National Institute of Technology (NIT), Durgapur, India, in 2011 and 2016, respectively. He received the scholarship from the Ministry of Human Resource and Development (MHRD), Government of India, for the M.Tech. degree, from 2009 to 2011, and the Ph.D. degree, from 2012 to 2016. He joined the Department of Electronics and Communication Engineering (ECE), NIT, Warangal, as an Assistant Professor, in April 2018. He has published more than 50 research papers in peer-reviewed international journals and conferences. His research interests include the analysis and synthesis of radiation pattern of time-modulated antenna array structures, evolutionary optimization techniques, the applications of soft computing in electromagnetics, RF, and microwaves, and soft computing techniques.

DURBADAL MANDAL (Member, IEEE) received the B.E. degree in electronics and communication engineering from Regional Engineering College, Durgapur, India, in 1996, and the M.Tech. and Ph.D. degrees from the National Institute of Technology (NIT), Durgapur, in 2008 and 2011, respectively. He is currently an Associate Professor with the Department of Electronics and Communication Engineering, NIT. He has published more than 300 research papers in international journals and conferences. His research interests include array antenna design and filter optimization through evolutionary computing techniques.